Computational Study of the Reactions of BH_2^+ with H_2, Methane, Ethane, Ethylene, and Acetylene in the Gas Phase

Xia Zeng and Gustavo E. Davico*

Department of Chemistry, University of Idaho, Moscow, Idaho 83844-2343

Received: August 11, 2003; In Final Form: October 8, 2003

We have studied the potential energy surface for the reactions of BH_2^+ with H_2, methane, ethylene and acetylene at the CCSD(T)/cc-pVTZ//MP2(full)/cc-pVTZ level and the reaction of BH_2^+ with ethane at the CCSD(T)/6-311G(d,p)//MP2(full)/6-311G(d,p) level of theory. A complete survey of the potential energy surfaces is presented and the structures of the stationary points and the mechanisms of these reactions are discussed. The calculations suggest that the products of these reactions are formed by addition and elimination of a hydrogen molecule, effectively activating the carbon−hydrogen bond. Furthermore, theory also suggests that elimination of HD is the sole product in the reaction of BD_2^+ with ethane; however, H/D scrambling occurs to some extent in the reaction with acetylene whereas it is complete in the reaction with ethylene. Therefore, loss of H_2, HD, and D_2 is predicted, in agreement with experiments. In addition, elimination of CH_4 can also be produced in the reaction of BH_2^+ with ethane, even with BD_2^+ as reactant. Although the products of the carbon−carbon bond activation are also exothermic in the reactions of acetylene and ethylene, they are prevented kinetically. The remarkable electrophilic properties of BH_2^+ are presented and discussed as well as details on the bonding structure of the three-center two-electron bonds characteristic of these compounds.

Introduction

The reactions of BH_2^+ with hydrogen and simple hydrocarbons have been the focus recently of several experimental and theoretical reports. Experimental results reported by DePuy et al.[1] include reactions with H_2, CH_4, C_2H_2, C_2H_4, C_2H_6, as well as H_2O, H_2S, and NH_3 by using a flowing afterglow-selected ion flow tube instrument. In addition, these authors also reported some reactions involving deuterium labeled reactants (BD_2^+ and/or labeled neutrals) that showed some insights on the reaction mechanisms. Furthermore, the reaction of BH_2^+ with an excess of H_2 was shown[1,2] to produce BH_6^+, a structure isoelectronic with CH_6^{2+} containing two three-center two-electron (3c−2e) bonds, which was the focus of substantial theoretical interest.[3,4] However, one of the main conclusions of these experiments was the observation that BH_2^+ can activate C−H and C−C bonds in hydrocarbons very efficiently, something that was thought to be just in the realm of transition metal cation chemistry[5,6] and of central importance in catalysis. The chemistry of BH_2^+ was found analogous to that of CH_3^+, despite BH_2^+ being isoelectronic with CH_2^{2+}; however, these experiments and theoretical results suggest significant differences in their reactivities,[1] consistent with a lower electrophilicity and increased selectivity of BH_2^+.

Kemper et al.[7] also studied the reaction of the ground state of B^+ ($^1S_0$) with H_2 and the H−H bond activation to form BH_2^+, which early theoretical results[8] predicted to be around 77 kcal/mol, showing that the addition of two weakly bound H_2 ligands reduces the barrier to almost zero. The cooperative interaction of the H_2 molecules was also proved by theory.[7,9] In a related experiment reported by Ranatunga et al.[10] a disubstituted boron cation ($CH_3BCH_3^+$ and $CH_3OBOCH_3^+$) breaks C═O and C−C bonds in aldehydes and ketones via −H or $-CH_3$ shift, similar to the reaction of BH_2^+ with ethane where the carbon−carbon bond is broken.

Some theoretical results on these reactions were also reported. The experimental results DePuy et al. also included calculations on the reaction with H_2 and CH_4 (including the structures of BH_4^+ and BH_6^+), and a portion of the potential energy surface of the reaction with C_2H_6.[1,2] It has also been shown that the complex BH_4^+ is a very strong Lewis acid and has very high electrophilicity. Calculations suggest that BH_4^+ readily forms complexes with CO_2, CS_2, and COS.[11] All of those adducts contain 3c−2e bonds and are 26−42 kcal/mol more stable than their reactants. McDonald et al. performed a detailed study of the CHB bridge bonding in $H_2CH_2BH_2^+$ using molecular orbital theory,[12] indicating that there are two 3c−2e bonds in this molecule. Qu et al. reported a potential energy survey for the reaction of BH_2^+ with C_2H_4 at the CCSD(T)/6-311G(2df,p)//B3LYP/6-311G(d,p) level;[13] however, several stationary points were missed in this report. Furthermore, it seems that the 3c−2e bond structures are very dependent on how much of the electron correlation is accounted for, as revealed by some substantial differences in some of the structures when compared with our MP2(full)/cc-pVDZ results. In addition, it is clear that the quality of the basis set might also play a role. Similar deficiencies are found in the potential energy surface for the reaction of BH_2^+ with C_2H_2 reported by the same authors.[14] In addition, Olah and co-workers recently reported calculations on a series of BH_2^+ reactions with neutrals containing double bonds including C_2H_4 and C_3H_6, as well as H_2CO and H_3CCHO; however, they focused only on a minuscule part of the potential energy surface, which included only the initial reaction complex and a hydride transfer process.[15]

Finally, the reactions of Al^+ with H_2 and small hydrocarbons were also reported recently[16] in an attempt to investigate the possibility of insertion of this ion, isovalent with B^+. However, the experiments failed to obtain $HAlH^+$ and calculations suggest

* Corresponding author. E-mail: davico@uidaho.edu.

10.1021/jp036386s CCC: $25.00
Published on Web 11/27/2003

TABLE 1: Energies, Symmetries, and Number of Imaginary Frequencies for the Reaction of BH_2^+ with H_2

species	symmetry	N_{imag}[a]	MP2(full)/cc-pVTZ (hartree)	CCSD(T)/cc-pVTZ[b] (hartree)	ZPE[c] (kcal/mol)	rel energy[d] (kcal/mol)
BH_2^+	$D_{\infty h}$	0	−25.55864	−25.56494	11.29	
H_2	$D_{\infty h}$	0	−1.16465	−1.17231	6.48	
$BH_2^+ + H_2$	N/A	N/A	−26.72329	−26.73725	17.77	0
1a	C_{2v}	0	−26.75462	−26.76701	22.90	−13.5
1tsaa′	C_{2v}	1	−26.72805	−26.73980	21.25	1.9
1tsb	C_{2v}	1	−26.74429	−26.75727	21.37	−9.0

[a] Number of imaginary frequencies. [b] Single point calculation at the MP2(full)/cc-pVTZ level optimized geometry. [c] Unscaled zero point vibrational energy from MP2(full)/cc-pVTZ level. [d] Relative energy at the CCSD(T)/cc-pVTZ//MP2(full)/cc-pVTZ level including ZPE.

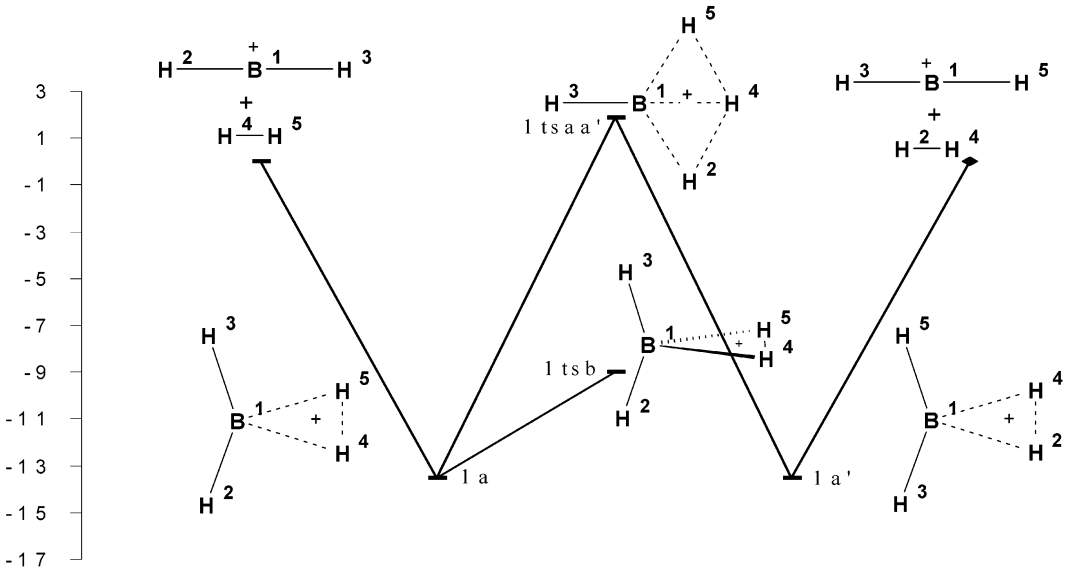

Figure 1. Potential energy surface and structures for the reaction of BH_2^+ with H_2 at the CCSD(T)/cc-pVTZ//MP2(full)/cc-pVTZ level including ZPVE.

that the formation of this ion from Al^+ and H_2 is endothermic, despite the fact that it is a minimum in the potential energy surface. As in the case of boron, cooperative effects of multiple H_2 molecules interacting with the Al^+ ion affected the reaction reducing slightly the endothermicity. The marked decrease in reactivity in Al^+ seems to be related to the size of the 3s orbital that prevents the approach of the ligands and the lack of low lying unoccupied orbitals, which make boron unique.

In this paper a systematic study and comprehensive comparisons on the title reactions are performed. A thorough potential energy survey is presented for all the reactions using high level ab initio calculations. We also explored the bonding nature of some of these compounds with emphasis on structures with 3c−2e bonds using the atoms in molecules (AIM) approach[17,18] and natural orbital (NO) analysis.[19]

Experimental Section

All calculations were performed with the Gaussian 98 suite of programs.[19] The geometry optimizations and frequency calculations as well as zero point energies (ZPE, not scaled) for the reactions of BH_2^+ with H_2, CH_4, ethylene, and acetylene were carried out at the MP2(full)/cc-pVTZ level. For improved energies, single-point calculations were performed at the CCSD(T)/cc-pVTZ//MP2(full)/cc-pVTZ level. Because of its size, in the reaction of BH_2^+ with ethane, the energies, frequencies, and ZPE (not scaled) were computed at the CCSD(T)/6-311G(d,p)//MP2(full)/6-311G(d,p) level due to software limitations and prohibitive CPU times that prevented the use of correlation consistent basis sets. The geometry of each stationary point was completely optimized at the appropriate level of theory within the reported symmetry. The number of negative eigenvalues in the Hessian was used to determine if a structure is a minimum, transition state, or higher order saddle point. IRC calculations at MP2(full)/6-311G(d,p) were performed for all the transition states to ensure that they connect the reported minima. Unless stated otherwise, the AIM analyses were performed at the MP2-(full)/cc-pVTZ level, and included up to d orbitals.[20] The topology of the density was also analyzed by plotting the density including all the orbitals and showed no significant differences with the AIM results in the location and structure of the critical points and bond critical paths.

Results and Discussion

The energies are reported relative to the infinitely separated reactants BH_2^+ and X (X = H_2, CH_4, C_2H_2, C_2H_4, C_2H_6) for each reaction. On the potential surfaces, atoms are labeled numerically conforming to certain pathways, but the labeling cannot be consistent to all of the reaction paths where an exchange of hydrogen atoms occurs.

$BH_2^+ + H_2$. The results for this reaction are listed in Table 1, which includes the energies and symmetries of different stationary points on the potential energy surface, and Figure 1, a plot of the potential energy surface including the structures of the stationary points. A complete discussion of this potential energy surface can be found elsewhere,[1] which involves a variety of theoretical methods including G2 (for all stationary points) and CBS-Q (for minima only), and is in excellent agreement with our results. Furthermore, the energies show little variability for the different theoretical methods. For these reasons, only a brief outline is given here before discussing the structure of the 3c−2e bonds.

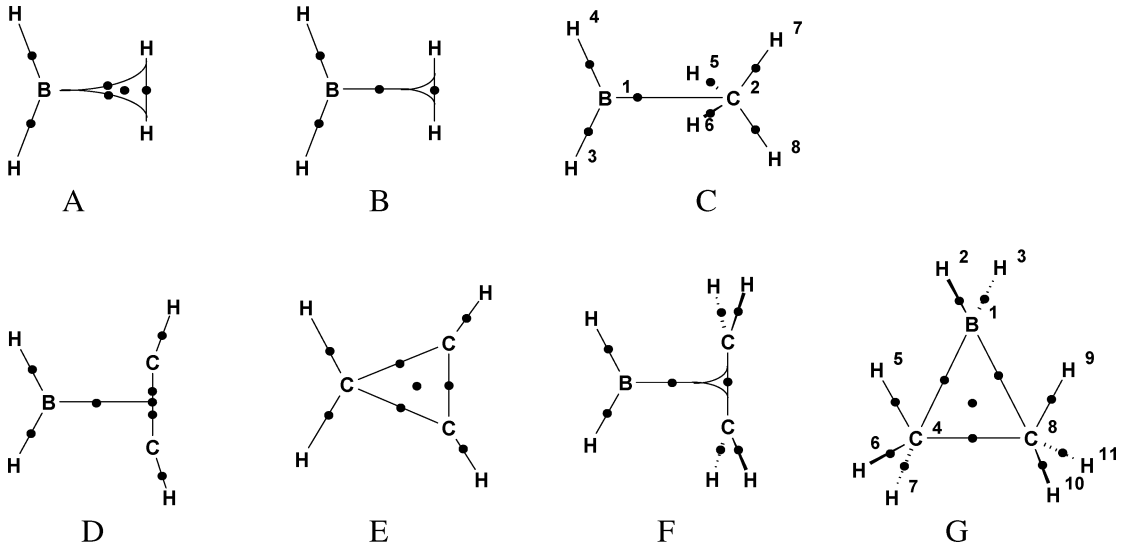

Figure 2. AIM analysis of BH_4^+ and other adducts. Dots represent approximate locations of critical points.

From Figure 1 it is clear that the reaction of BH_2^+ with H_2 leads to the formation of BH_4^+ (**1a**), a 13.5 kcal/mol exothermic process. In most encounters, this intermediate dissociates back to reactants; however, a small fraction could have the required energy to surmount the transition state **1tsaa′** to produce **1a′**, in which the position of two hydrogen atoms are exchanged. From there the process can be repeated and a double exchange is possible. Interestingly, the ZPE plays a very important role in the potential energy surface. The complex **1a** (**1a′**) is 18.7 kcal/mol more stable than the reactants (products) when only electronic energies are considered at the CCSD(T)/cc-pVTZ//MP2(full)/cc-pVTZ level. This binding energy decreases to 13.5 kcal/mol when the ZPE is included (Table 1), in excellent agreement with the 14.7 ± 0.5 kcal/mol value obtained experimentally.[7] The approximate 5 kcal/mol difference in energy might account for the inconsistency found by Sharp[9] when comparing their value to the experimental and early theoretical[1] results. In comparison to reactants or products, the complex has more vibrational normal modes. Moreover, the new normal modes of the complex have very small reduced masses whereas the bonding characteristic in the H_2 molecule does not change substantially, and therefore the ZPE increases dramatically. The contribution of ZPE also raises the energy of **1tsaa′** to 1.9 kcal/mol above the reactants, as shown in Figure 1. For most of the reactions discussed in this report the final step is the dissociation of this type of complex. Thus it is necessary that all the relative energies include ZPE. However, this effect should be less pronounced with the other reactions involving heavier neutrals.

Minimum **1a** has a planar structure with a 3c−2e bond. The bond length of B^1-H^5 in **1a** is 1.42 Å, longer than the 1.17 Å of the B^1-H^3 bond. The rotation of H^4-H^5 in **1a** leads to transition state **1tsb**, in which the H^4-H^5 moiety is perpendicular to the $H^2-B^1-H^3$ plane. But the 3c−2e bond still exists in this geometry. The energy barrier for this rotation is 4.6 kcal/mol at the CCSD(T)/cc-pVTZ//MP2(full)/cc-pVTZ level. This value is small compared to the barrier for the isomerization of **1a** to **1a′** through transition state **1tsaa′**, which lies 15.4 kcal/mol above **1a** and 1.9 kcal/mol above reactants. The relatively high energy of this transition state in the potential energy surface, which switches the positions of H^5 and H^2, plays an important role in the isotopic reaction described later. In addition, it provides enough lifetime for adduct **1a** to collide with the He buffer gas in the flowing afterglow instrument removing its excess energy and trapping it in the deep potential well, thus enabling it to reach the detector.

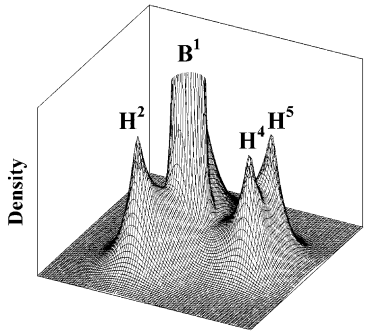

Figure 3. Electron density of **1a** in the molecular plane calculated at the MP2(full)/cc-pVDZ level.

The structure of the $B-H_2$ 3c−2e bond in BH_4^+ is observed in several complexes in the series of reactions discussed here. The 3c−2e bond is normally described as three bonds forming a cyclic structure.[1,2,9,11,21−23] The AIM analysis at MP2(full)/6-311G(d,p) level indicates that there are three bond critical points and one ring critical point (see A in Figure 2), which agrees with the classical structure. However, at the MP2(full)/cc-pVTZ level the bonding structure is slightly different (see B in Figure 2); both B−H bonds collapse partially along the axis connecting the boron atom and the center of the H_2 bond and the ring critical point disappears. However, the B−H bonds still exist, though they exhibit strong bond curvature, making the bond critical paths substantially longer than the distance between these attractors. To check for convergence in the electron density, BH_4^+ was re-optimized using a quadruple-ζ basis set, and we found that this structure persists even at the MP2(full)/cc-pVQZ level. Figure 3 shows the total electron density of **1a** in the molecular plane. In this figure, in which the attractors are clearly observed and have also been labeled, a saddle point on the electron density surface represents a bond critical point and a local minimum represents a ring critical point. This plot shows clearly that only a saddle point is found in the area between boron and H^4-H^5. Despite the fact the 6-311G(d,p) basis set predicts the energetics of this reaction adequately[1] (and is used later in this article), it may not be complete enough to be able to describe the 3c−2e bonding in **1a** adequately.

The NO analysis reveals a direct bonding between the σ bond in H_2 and a vacant sp^2 orbital localized on the boron atom along

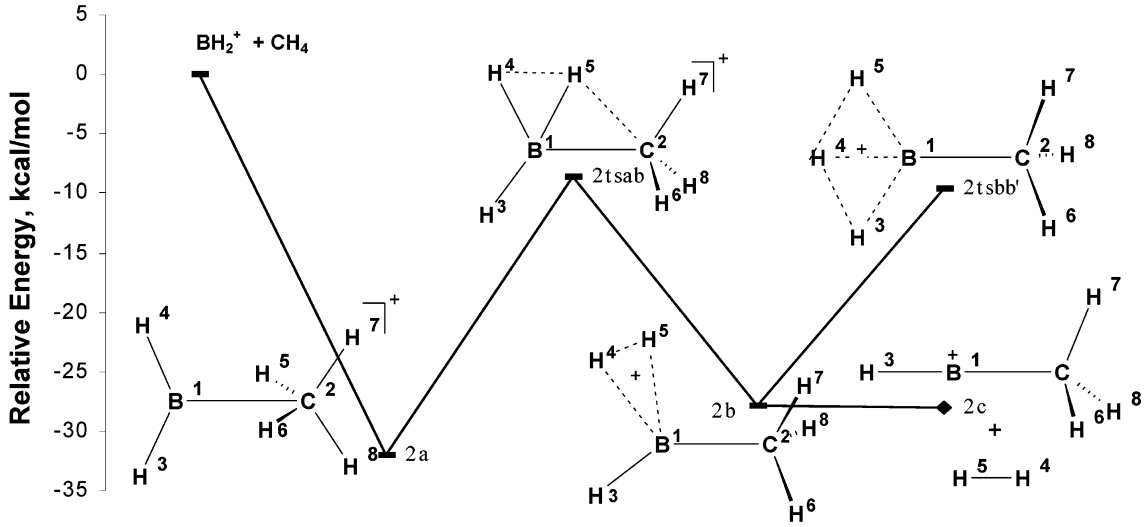

Figure 4. Potential energy surface and structures for the reaction of BH_2^+ with CH_4 at the CCSD(T)/cc-pVTZ//MP2(full)/cc-pVTZ level including ZPVE.

TABLE 2: Energies, Symmetries, and Number of Imaginary Frequencies for the Reaction of BH_2^+ with CH_4

species	symmetry	N_{imag}[a]	MP2(full)/cc-pVTZ (hartree)	CCSD(T)/cc-pVTZ[b] (hartree)	ZPE[c] (kcal/mol)	rel energy[d] (kcal/mol)
CH_4	T_d	0	−40.42799	−40.43799	28.61	
2c	C_{3v}	0	−64.85959	−64.86780	28.74	
$BH_2^+ + CH_4$	N/A	0, 0	−65.98663	−66.00293	39.91	0
2a	C_{2v}	0	−66.04714	−66.05942	43.27	−32.1
2tsab	C_s	1	−66.00488	−66.01685	40.09	−8.5
2b	C_1	0	−66.03432	−66.04831	40.48	−27.9
2c + H_2	N/A	0, 0	−66.02424	−66.04011	35.22	−28.0
2tsbb′	C_s	1	−66.00542	−66.01820	39.96	−9.5

[a] Number of imaginary frequencies. [b] Single point calculation at the MP2(full)/cc-pVTZ level optimized geometry. [c] Unscaled zero point vibrational energy from MP2(full)/cc-pVTZ level. [d] Relative energy at the CCSD(T)/cc-pVTZ//MP2(full)/cc-pVTZ level including ZPE.

the B−H_2 axis, the 3c−2e bond, in agreement with the AIM results. Furthermore, the fact that this interaction is mainly localized along this axis is also supported by the energetic of the H^4−H^5 rotation. The barrier for rotation of H_4−H_5 in **1a** around this axis is only one-third of its binding energy suggesting that no major interaction is compromised upon rotation. Our NO analysis suggests that the origin of this barrier is due to a weak interaction between the occupied B−H σ bonds in BH_2^+ with the H_2 σ* orbital. This electron donation back to H_2 was also suggested by DePuy[1] on the basis of MO analysis.

DePuy et al. also studied experimentally the isotopic reaction of BH_2^+ with D_2.[1] Because the rate-limiting transition state **1tsaa′** lies slightly higher in energy than the reactants, BH_2^+ reacts inefficiently with D_2 to produce products BHD^+ and BD_2^+. They reported that the efficiency for this reaction[1] is 0.030, which is very small compared to the efficiency of the reaction of BH_2^+ with methane, acetylene, ethylene, and ethane, as will be discussed later. The efficiency is the ratio of the experimental rate constant to the collision rate and is a measure of the fraction of collisions that goes over the barrier to yield products; thus the larger the efficiency the larger the fraction of collisions that leads to products. The collision rates for nonpolar neutral reagents are calculated as Langevin rate constants,[24] and those for polar reagents are theoretical ADO rate constants.[25] The major product for this reaction is BHD^+ (91%)[1] and the transition state **1tsaa′** is involved in the H/D exchange. From **1a** to **1a′**, the 3c−2e bond switches from B^1−H^5−H^4 to B^1−H^4−H^2, leading to the loss of H^2−H^4. BD_2^+, the product of a double H/D, is found in very small amounts (9%) because overcoming the high barrier of **1tsaa′** again is required to complete the second exchange, which is unfavorable with respect to dissociation to BHD^+. The experimental result fits the calculated potential energy surface very well (Figure 1). As mentioned before, transition state **1tsb** leads to the rotation of H^4−H^5, it is 10.9 kcal/mol more stable than **1tsaa′** and therefore rotation of H^4−H^5 should occur much faster than the switching of the 3c−2e bond; however, it does not contribute to the H/D scrambling. The reaction of BD_2^+ with H_2 gave similar experimental results and revealed a small primary kinetic isotope effect.

BH_2^+ + CH_4. The potential energy surface for the reaction of BH_2^+ with CH_4 is presented in Figure 4 and data on the stationary points are listed in Table 2. In general, our high level calculations agree qualitatively with the MP2(full)/6-311G(d,p) results reported earlier.[1] Two minima, **2a** and **2b** are found on the potential energy surface. The initial adduct **2a** is a structure with C_{2v} symmetry that lies in a relatively deep potential well. This is a very interesting structure that can be considered as a very simple carborane and requires additional scrutiny.

Compound **2a** lies 32.1 kcal/mol below the reactants. The interaction energy is substantially larger than a typical 10−20 kcal/mol found in electrostatic complexes. Our AIM analysis indicates a strong covalent bonding showing a bond critical point between the boron and carbon atoms. In addition, we also found bonding between carbon and hydrogen atoms whereas no bond exists between boron and the bridging hydrogen atoms (see C in Figure 2). This is in disagreement with interpretations by McDonald et al.[12] based on canonical MO analysis, which suggested that the carbon and boron atoms share the bridging hydrogen atoms, indicating that in **2a** H^5 and H^6 approach B^1

and form two 3c−2e bonds: $B^1H^5C^2$ and $B^1H^6C^2$. Our NO analysis is also inconsistent with a bond connecting boron and the bridging hydrogen atoms in **2a**. Instead, it shows a direct interaction of the rehybridized BH_2^+ sp^2 orbital with the carbon atom, in agreement with the AIM results. In addition, a weak interaction between the bridging hydrogen atoms and the empty π orbital in BH_2^+ is observed, similar to the back-bonding type of interaction found in BH_4^+. As in the case of the reaction with H_2, this interaction represents only about one-third of the total association energy, as calculated by rotating the BH_2 moiety in **2a** 90°. Comparing the differences in structure between **2a** and reactants also supports the marginal involvement of the bridging hydrogen atoms in its bonding scheme, which interestingly was also noted by McDonald.[12] Although the $H^5-C^2-H^6$ angle increases by 8°, the C^2-H^5 (or C^2-H^6) bond length increases by only 0.05 Å. As a comparison, the increased C−H bond length represents an elongation of about 4% with respect to CH_4 whereas in the reaction with H_2 the H−H bond length increases by 10%. This suggests that the C−H bonds in the CH_4 moiety of **2a** are not appreciably distorted with respect to isolated CH_4, with the increased H−C−H angle offering only enough space for the boron to attack the carbon atom. In addition, the small C−H bond length increase can be explained by the weak electron donation from the bridging hydrogen atoms to the empty π orbital localized on the boron atom discussed above. As a result, the structure of **2a** is shown as depicted in Figure 4, with an almost formal bond between the carbon and boron atoms.

Minimum **2b** is a structure with C_1 symmetry analogous to **1a**. The H_2 molecule in **2b** is very weakly bound with respect to products (only 0.1 kcal/mol). Thus when **2b** is formed through transition state **2tsab**, dissociation occurs very quickly. Although the transition state connecting **2a** and **2b**, **2tsab**, is 23.5 kcal/mol above adduct **2a**, it lies 8.5 kcal/mol below the reactants; therefore, this reaction should occur faster than the reaction of BH_2^+ with H_2. As discussed later, experimental results agree with this observation.[1] The 3c−2e bond in **2b** can switch from $B^1-H^4-H^5$ to $B^1-H^3-H^4$ through a transition state **2tsbb′**, which was included in our calculations because, as in the previous reaction, it could be relevant in deuterium labeled reactions.

Compound **2c**, an ion with C_{3v} symmetry, is obtained by substitution of one of the hydrogen atoms in BH_2^+ by a methyl group. This substitution does not change the geometry around the boron atom considerably; however, it affects the electrophilicity of the cation substantially. As mentioned before and shown in Figure 4, the reaction of **2c** with H_2 is essentially thermoneutral whereas the reaction of BH_2^+ with H_2 is exothermic by 13.5 kcal/mol (Figure 1). A similar situation occurs with methane. Bell et al.[26] reported that the reaction of CH_4 with **2c** is analogous to the reaction of CH_4 with BH_2^+. Both reactions produce very similar adducts, but the binding energy of the former reaction (12.6 kcal/mol) is much smaller than the latter one (32.1 kcal/mol) due to the electron donating characteristic of the methyl group.

The validity of the potential energy surface can be scrutinized by further experiments. As discussed before,[1] the switching reaction shown in eq 1 can be used for this purpose because it

$$BH_4^+ + CH_4 \rightarrow H_4C-BH_2^+ + H_2 \qquad (1)$$

generates **2a** from a less exothermic process. In this reaction, **2a** has only 18.6 kcal/mol (see Tables 1 and 2) excess energy instead of 32.1 kcal/mol from the direct reaction of BH_2^+ and CH_4. Therefore, even if all the excess energy remains in **2a**, it is not sufficient to surmount **2tsab** and proceed to products, in excellent agreement with experiments.

The efficiency for the reaction of BH_2^+ with CH_4 is 0.64,[1] substantially larger than the one reported for the reaction of BH_2^+ with H_2. Our calculations indicate that the overall rate-limiting step involves transition state **2tsab**, which is 8.5 kcal/mol more stable than the reactants, consistent with the measured reaction efficiency.

The isotopic reactions of BD_2^+ with CH_4 and BH_2^+ with CD_4 lead to the exclusive loss of HD, in striking contrast with the reaction of CH_3^+ with CD_4 (or CD_3^+ with CH_4), where almost complete scrambling occurs.[1] By following the reaction path and the structures shown in Figure 4, it can be clearly seen that in the product hydrogen molecule, H^4-H^5, one hydrogen originates from BH_2^+ and the other one comes from CH_4. These theoretical results compare very well with the experiments. We should also mention that in transition state **2tsbb′**, the 3c−2e bond switches between $B^1-H^4-H^5$ and $B^1-H^4-H^3$, leading to the exchange of H_3 and H_5 in complex **2b** and possible H/D scrambling in the labeled reactions. However, compared to products, **2tsbb′** is 18.5 kcal/mol higher in energy and therefore **2b** dissociates directly rather than going first through **2tsbb′**. As a consequence, exclusive loss of HD occurs in this reaction, in agreement with experiments.

$BH_2^+ + C_2H_2$. The results for this reaction are shown in Figure 5 and listed in Table 3. This reaction was studied experimentally by DePuy,[1] and some insights into the potential energy surface were reported recently by Qu et al.[14]

The reaction of BH_2^+ with C_2H_2 leads initially to the formation of adduct **3a**. This structure is located in a very deep potential energy well, which is 61.4 kcal/mol lower than the reactants. In principle, the release of such energy could be rationalized in terms of the interaction between the electron deficient BH_2^+ and the electron rich C_2H_2 fragments. Compound **3a** is a structure with C_{2v} symmetry in which all the atoms are in the same plane. With such a structure, it should be expected that BH_2^+ would interact with one of the acetylene π bonds to form a 3c−2e bond and perhaps that the other, orthogonal, π bond could extend to the boron atom to form a two electron aromatic type of delocalized π orbital that would contribute to its stability. The analysis based on the canonical MO of **3a** seems to confirm this structure, indicating a strong interaction between an empty orbital localized on the boron atom with the in-plane carbon−carbon π bond as well as an aromatic type of orbital. In addition, the back-bonding of the B−H bonds in BH_2^+ into the acetylene in-plane π^* orbital is also clear, which is analogous to the interaction observed in adduct **1a** in the reaction of BH_2^+ with H_2. Results from the NO analysis also indicate the lack of direct interaction (σ bonds) between the boron and the carbon atoms, suggesting that there is no cyclic structure but instead a "T" shaped bond connecting the boron atom with the center of the carbon−carbon bond. However, NO analysis shows that there is no delocalized π orbital. AIM analysis also supports these results, and, as indicated in Figure 2D, it seems that carbon and boron atoms do not form a cyclic structure because no ring critical point is found. Instead, boron is connected to C^2-C^3 by a bond that extends to the center of the C^2-C^3 bond. This is a very interesting topology, which seems to be more associated with transition states than minima. There are three critical points along the C^2-C^3 bond: the center one is a local maximum or attractor, and the other two are located at each side and are bond critical points. The values of the density at these points are similar; however, this peculiar structure was confirmed by inspecting a plot of the total density

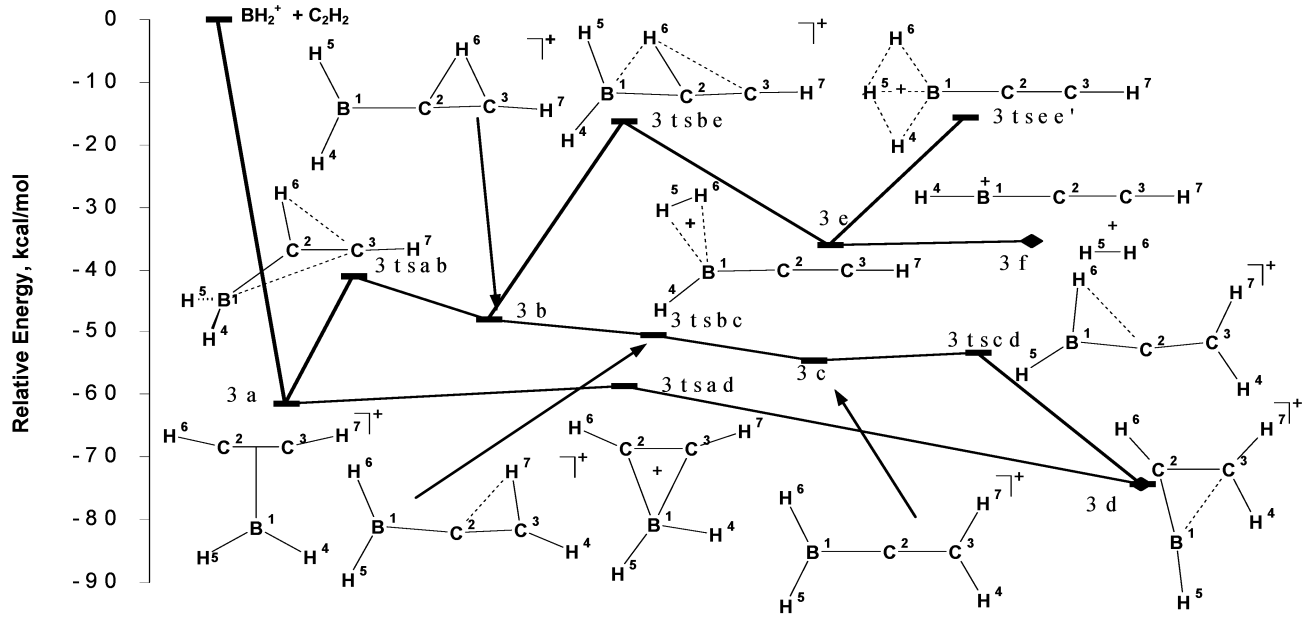

Figure 5. Potential energy surface and structures for the reaction of BH_2^+ with C_2H_2 at the CCSD(T)/cc-pVTZ//MP2(full)/cc-pVTZ level including ZPVE.

TABLE 3: Energies, Symmetries, and Number of Imaginary Frequencies for the Reaction of BH_2^+ with C_2H_2

species	symmetry	N_{imag}[a]	MP2(full)/cc-pVTZ (hartree)	CCSD(T)/cc-pVTZ[b] (hartree)	ZPE[c] (kcal/mol)	rel energy[d] (kcal/mol)
C_2H_2	$D_{\infty h}$	0	−77.18869	−77.18758	16.75	
3f	$C_{\infty v}$	0	−101.63852	−101.63287	19.05	
$BH_2^+ + C_2H_2$	N/A	0, 0	−102.74733	−102.75252	28.03	0
3a	C_{2v}	0	−102.85500	−102.85568	31.40	−61.4
3tsab	C_s	1	−102.80902	−102.81943	28.96	−41.1
3b	C_s	0	−102.82783	−102.83213	29.95	−48.1
3tsbe	C_s	1	−102.77877	−102.77820	27.91	−16.2
3e	C_s	0	−102.81118	−102.81245	29.71	−35.9
3f + H_2	N/A	0, 0	−102.80317	−102.80518	25.53	−35.6
3tsbc	C_s	1	−102.82641	−102.83507	29.23	−50.6
3c	C_{2v}	0	−102.83000	−102.84269	30.00	−54.6
3tscd	C_s	1	−102.82800	−102.84035	29.78	−53.4
3d	C_s	0	−102.87806	−102.87901	32.97	−74.4
3tsad	C_s	1	−102.85042	−102.85098	31.08	−58.7
3tsee′	C_{2v}	1	−102.77808	−102.77879	28.97	−15.6

[a] Number of imaginary frequencies. [b] Single point calculation at the MP2(full)/cc-pVTZ level optimized geometry. [c] Unscaled zero point vibrational energy from MP2(full)/cc-pVTZ level. [d] Relative energy at the CCSD(T)/cc-pVTZ//MP2(full)/cc-pVTZ level including ZPE.

in the molecular plane. Further insights into the structure of this adduct can be obtained by rotating the BH_2 moiety in **3a** by 90°. We found that this process requires only 23.1 kcal/mol at MP2(full)/6-311G(d,p) level, about one-third of the total reaction energy, indicating that the main interaction between the reactants is located along the C_{2v} axis. In addition, it is interesting to compare the AIM results with what is found for $C_3H_4^{2+}$, also a planar structure isoelectronic with **3a**. The results, shown in Figure 3E, reveal that $C_3H_4^{2+}$ has a structure very different from that of **3a**, with three bond critical points and one ring critical point indicating its cyclic nature. We attribute the difference to the lower electrophilicity of BH_2^+ that prevents its interaction with the carbon atoms of acetylene strongly enough to form sigma bonds. The substantially longer boron−carbon distance in **3a** also supports this conclusion.

As seen in Figure 5, **3a** can rearrange to **3b** through transition state **3tsab**. This transition state has C_s symmetry and all the atoms except for H^4 and H^5 are on one plane. According to the calculations of Qu et al.,[14] this transition state is predicted at the B3LYP/6-311G(d,p) level to have all the atoms on one plane. Our results at the MP2(full)/cc-pVTZ level show that the totally planar structure has two imaginary frequencies.

From **3b** two energetically feasible pathways are calculated, as shown in Figure 5. The higher energy path leads to the loss of a hydrogen molecule. On this path, H^6 shifts to B^1 forming complex **3e** through **3tsbe**. Similar to complex **2b**, **3e** has a weakly bound H_2 molecule and dissociates very fast to generate linear product **3f** and H_2. The 3c−2e bond in **3e** can switch from $B^1-H^4-H^5$ to $B^1-H^5-H^6$ through transition state **3tsee′**; however, it is 20 kcal/mol higher in energy than the products. Therefore, complex **3e** dissociates readily to **3f** and H_2 without exchanging the position of the hydrogen atoms. In addition, the dissociating products are favored entropically.

On the other reaction path, H_6 in **3b** shifts now to the opposite direction and forms minimum **3c**. The transition state connecting **3b** and **3c** is **3tsbc**. In contrast to the calculation at MP2(full)/6-311G(d,p) and MP2(full)/cc-pVTZ levels in which the energy of **3tsbc** is higher than **3b** and **3c** (see Table 3), the results at the CCSD(T)/cc-pVTZ//MP2(full)/cc-pVTZ level show that the barrier between **3b** and **3c** disappears and **3b** becomes unbound

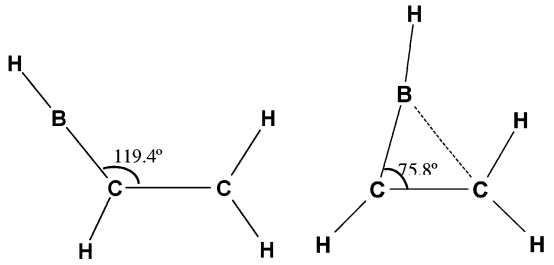

A B

Figure 6. Structure of **3d** at (A) B3LYP/6-311G(d,p) and (B) MP2-(full)/cc-pVDZ level.

even without considering the ZPE. Inclusion of the ZPE increases this difference making **3tsbc** even more stable. Clearly this portion of the potential energy surface is quite flat and its structure depends on the basis set and the method employed; however, our best theoretical method indicates that **3tsbc** is not a stationary point, in agreement with DFT results by Qu and co-workers.

H_6 in **3c** can shift from B^1 to C^2 to form minimum **3d**. This is the most stable structure in the potential energy surface. The structure of **3d** has been described earlier by Qu et al.[13] In their B3LYP/6-311G(d,p) calculation **3d** has a structure resembling the allyl cation (see Figure 6). However, in our higher level calculation B^1 is closer to C^3 and a weak interaction between these centers is evident. The B^1-C^3 bond length is about 1.7 Å, larger than the 1.4 Å of the B^1-C^2 bond in the same compound. Despite the fact that the potential energy surface appears to be very flat in this area, it seems that results at the B3LYP/6-311G(d,p) level produce an incorrect geometry.

Cyclic BC_2H_3 (Borirene) was reported as the smallest aromatic molecule.[27,28] Protonation of borirene generates **3d** or **3a**, depending on which atom the proton attaches to; however, it seems that protonation in either center disrupts its cyclic structure. The transition state between **3a** and **3d** (**3tsad**), which was also found by Qu,[14] lies very close in energy to **3a** (only 2.6 kcal/mol higher). Because the barrier for **3a**−**3b** is 20.3 kcal/mol, the isomerization of **3a** to **3d** should proceed much faster through **3tsad** than through **3tsab**−**3b**−**3tsbc**−**3c**−**3tscd**−**3d**. However, both paths are accessible because they are both more than 40 kcal/mol below reactants. In addition, it should be pointed out that the system should go first to **3b** to form **3f** and H_2, the only products observed experimentally.

The measured efficiency for this reaction is 1.00, indicating that products are formed in every collision.[1] Our theoretical results indicate that the rate-limiting transition state, **3tsbe**, is 16.2 kcal/mol more stable than the reactants. With such a low relative energy (and the large initial exothermicity), almost all collisions lead to products instead of going back to reactants, resulting in the high efficiency observed experimentally. Although there are a variety of very stable structures, like **3d**, almost 75 kcal/mol more stable than the reactants, once formed they proceed to products very quickly in comparison to their collision rate with the He buffer gas in the flowing afterglow instrument, and stabilization (and detection) of the adduct should not be favorable, in agreement with experimental results.

Experiments suggest that the reaction of BD_2^+ with C_2H_2 leads to the loss of H_2, HD, and D_2 in approximately a 1:2:1 (H_2:HD:D_2) ratio.[29] If isotope effects are neglected, which is reasonable for such a fast reaction, a statistical ratio of 1:4:1 would be expected for a total H/D scrambling process. Obviously, H/D scrambling occurs to some extent in this reaction yet not all the hydrogen and deuterium atoms become totally equivalent. Following the higher energy pathway in Figure 5, **3a**−**3tsab**−**3b**−**3tsbe**−**3e**−products, it can be seen that H_6 migrates from C^2 to B^1 to form complex **3e**. As in the reactions discussed above, transition state **3tsee′** cannot account for H−D scrambling because it is 20.3 kcal/mol higher in energy than **3e** and cannot compete with the almost thermoneutral dissociation to form products. Therefore, this pathway would eliminate exclusively HD in the reaction of BD_2^+ with C_2H_2. This pathway, as well as the totally random elimination, predicts that HD should be relatively more abundant than H_2 and D_2 suggesting that previous isomerization of **3a** should occur, for example, through the **3a**−**3tsad**−**3d**−**3tscd**−**3c**−**3tsbc**−**3b**−**3tsbe**−**3e**−product pathway. In this pathway, overcoming the transition state **3tsab** is replaced by a series of lower energy processes, as discussed before. The structure of compound **3c** is of crucial significance, because the linear $B^1-C^2-C^3$ moiety cannot rotate freely. Therefore, either H^7 shifts over to B^1 forming a $B^1-H^6-H^7$ 3c−2e bond in **3e** or H^4 shifts forming a $B^1-H^4-H^5$ 3c−2e bond in **3e**. The eliminated neutral species is H^6-H^7 or H^4-H^5, respectively, indicating that the isotopic reaction would lead to the loss of H_2 or D_2 in equal abundance. The **3a**−**3d** isomerization could occur many times back and forth before **3e** is obtained, either through **3tsab** or through **3b**−**3tsbc**−**3c**−**3tscd**. This process, in conjunction with the relatively low energy required to rotate the BH_2 moiety in **3a** discussed above, would result in a complete H/D scrambling. Clearly, this process occurs to some extent before **3tsbe**, the overall rate-limiting transition state, is surmounted.

$BH_2^+ + C_2H_4$. Similar to the reactions of BH_2^+ with CH_4 and C_2H_2, our theoretical results suggest that this reaction also proceeds by addition and elimination of a hydrogen molecule, in agreement with experiments.[1] The results are shown in Table 4 and Figures 7 and 8.

The relative energies calculated by CCSD(T)/cc-pVTZ//MP2-(full)/cc-pVTZ agree qualitatively with those calculated at the CCSD(T)/6-311G(2df,p)//B3LYP/6-311G(d,p) level by Qu et al.[13] However, because **4e** is identical to **3d,** its structure is predicted to be different by these two methods, as discussed above. In addition, these authors did not report a substantial portion of the potential energy surface including compound **4g**, the most stable structure.

As shown in Figure 7, adduct **4a** is 55.0 kcal/mol more stable than the reactants, a value slightly lower than that for **3a**, which is 61.4 kcal/mol below the entrance level. The difference in binding energy can be explained in terms of the electron density between the carbon atoms, which is lower in ethylene than in acetylene. Therefore, BH_2^+ interacts strongly with the latter.

As shown in Figure 2F, the results from the AIM analysis suggest that BH_2^+ attacks the ethylene π bond, and two boron carbon bonds are formed. However, these bonds have very curved bond critical paths and the bond critical points are located along the C_{2v} symmetry axis indicating, as in **1a** in the reaction with H_2, that most of the interaction is localized along that axis. The energy required to rotate the BH_2 moiety by 90° on the C_{2v} axis in **4a** is only 8.6 kcal/mol at the MP2(full)/6-311G-(d,p) level, which is consistent with the AIM results.

Starting from **4a**, the potential energy surface can be divided in four reaction pathways for analysis. The paths **4a**−**4tsad**−**4d**−**4e** and **4a**−**4tsad′**−**4d′**−**4e** have similar or related transition states and minima structures as well as energies because **4d** and **4d′** are two different conformers of the same compound. In **4d** $B^1-H^3-H^6$ forms a 3c−2e bond and eliminates H^3-H^6 upon dissociation. In contrast, **4d′** eliminates H^2-H^6 upon

TABLE 4: Energies, Symmetries, and Number of Imaginary Frequencies for the Reaction of BH_2^+ with C_2H_4

species	symmetry	N_{imag}[a]	MP2(full)/cc-pVTZ (hartree)	CCSD(T)/cc-pVTZ[b] (hartree)	ZPE[c] (kcal/mol)	rel energy[d] (kcal/mol)
C_2H_4	D_{2h}	0	−78.43000	−78.43858	32.43	
4e	C_s	0	−102.87806	−102.87901	32.97	
$BH_2^+ + C_2H_4$	N/A	0, 0	−103.98864	−104.00352	43.72	0
4a	C_{2v}	0	−104.08664	−104.09664	47.20	−55.0
4tsab	C_1	1	−104.05670	−104.06905	45.36	−39.5
4b	C_1	0	−104.06694	−104.08095	45.22	−47.1
4tsbc	C_1	1	−104.06438	−104.07895	44.90	−46.1
4c	C_s	0	−104.09904	−104.10887	47.46	−62.4
4tsce	C_1	1	−103.99941	−104.00992	43.71	−4.0
4e + H_2	N/A	0, 0	−104.04271	−104.05133	39.45	−34.3
4tsac	C_s	1	−104.07635	−104.08556	46.56	−48.6
4tsad′	C_1	1	−104.02836	−104.03708	44.54	−20.2
4d′	C_s	0	−104.05491	−104.06597	45.23	−37.7
4tsad	C_1	1	−104.01695	−104.02694	44.07	−14.3
4d	C_s	0	−104.05716	−104.06816	45.45	−38.8
4tscf	C_s	1	−103.96344	−103.97614	44.67	18.1
4f	C_s	0	−103.98659	−103.98659	46.79	13.7
4tsfg	C_1	1	−103.94075	−103.94075	44.75	40.4
4g	D_{3d}	0	−104.15154	−104.16356	46.65	−97.5
4tsdd′	C_s	1	−104.02792	−104.03783	44.62	−20.6

[a] Number of imaginary frequencies. [b] Single point calculation at the MP2(full)/cc-pVTZ level optimized geometry. [c] Unscaled zero point vibrational energy from MP2(full)/cc-pVTZ level. [d] Relative energy at the CCSD(T)/cc-pVTZ//MP2(full)/cc-pVTZ level including ZPE.

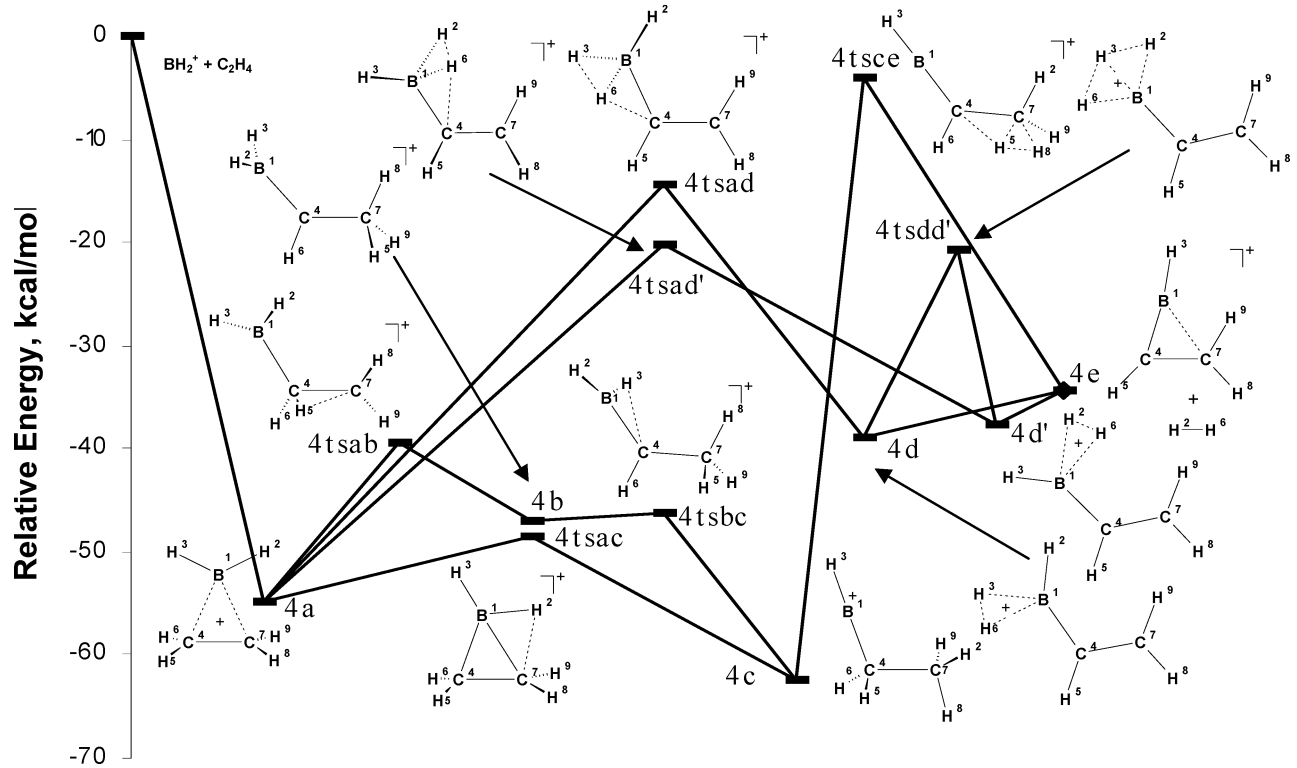

Figure 7. Potential energy surface and structures for the reaction of BH_2^+ with C_2H_4 at the CCSD(T)/cc-pVTZ//MP2(full)/cc-pVTZ level including ZPVE.

dissociation. In both cases one hydrogen atom originates from BH_2^+ and the other comes from C_2H_4. The transition state connecting **4a** and **4d, 4tsad**, is 5.9 kcal/mol higher than **4tsad′**, which connects **4a** and **4d′**. Therefore, the pathway **4a**−**4tsad′**−**4d′** products should be favored although **4d** is more stable than **4d′**. Furthermore, we should note that both transition states are more stable than the reactants and that, in principle, both could be involved in the reaction mechanism. The transition state **4tsdd′** connects **4d** and **4d′**, shifting the B−H−H 3c−2e bonds, and is energetically comparable to **4tsad′**; however, it cannot compete with the rapid dissociation to products from either **4d** or **4d′**.

The other two pathways, **4a**−**4tsac**−**4c**−**4tsce**−**4e** and **4a**−**4tsab**−**4b**−**4tsbc**−**4c**−**4tsce**−**4e**, share two stationary points, minimum **4c** and transition state **4tsce**. In the first pathway, H^2 in compound **4a** shifts from B^1 to C^7 and the B^1-C^7 and B^1-H^2 bonds break to form **4c** through **4tsac**. This reaction step is the only one reported by Olah et al. in their recent theoretical study of the reactions of BH_2^+ with alkenes at the B3LYP/6-311+G(d,p) level.[15] Their results agree with ours; however, the stability of structure **4a** seems to be overestimated by about 10 kcal/mol in their report. On the other path, the B^1-C^7 bond in **4a** breaks, going through transition states **4tsab** and **4tsbc** and minimum **4b** involving a series of hydrogen shifts (see Figure

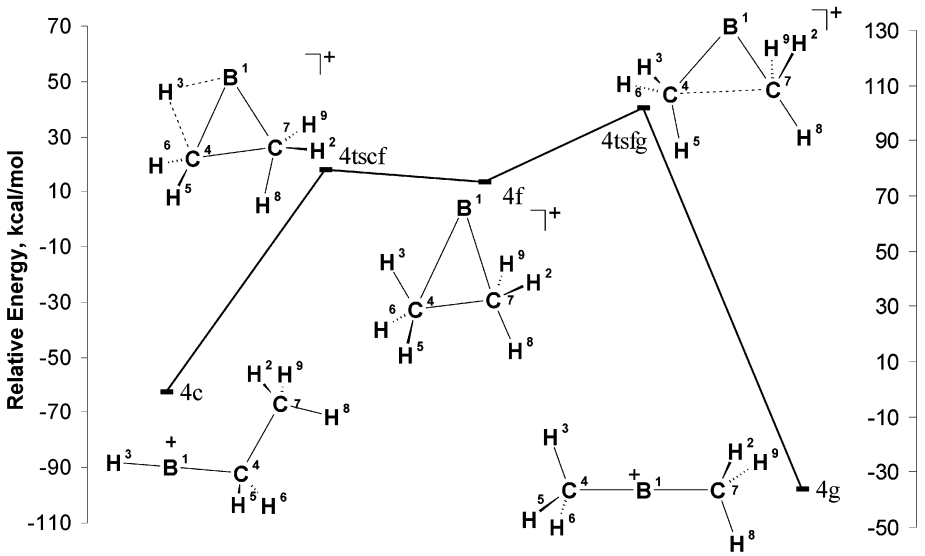

Figure 8. Potential energy surface and structures for the isomerization pathway between **4c** and **4g** at the CCSD(T)/cc-pVTZ//MP2(full)/cc-pVTZ level including ZPVE. The left axis is the energy relative to $BH_2^+ + C_2H_4$, and the right axis is relative to **4c**.

7) to form **4c**. In the portion shared by these two paths, transition state **4tsce**, which connects **4c** and **4e**, is 16.2 and 10.3 kcal/mol higher in energy than **4tsad′** and **4tsad**, respectively, the competing pathways to products. In comparison, although **4tsce** lies slightly below the reactant's energy, the higher energy barrier makes it unfavorable for **4c** to follow pathway **4c**−**4tsce**−**4e**. Instead **4c** must go back to **4a** through either **4tsac** or **4tsbc**−**4b**−**4tsab** (see Figure 7).

Compound **4c** is a very stable structure on the potential surface in which the ethyl group stabilizes the positive charge, similar to what is observed in **2c** and **3d**. Qu identified **4c** as the most stable minimum in the $[B,C_2,H_6]^+$ potential energy surface; however, it is easily predicted that two methyl groups should stabilize the positive charge in boron more than one ethyl group. Sure enough, as shown in Figure 8 and Table 4, structure **4g** is found to be about 35 kcal/mol more stable than **4c** and consequently about 100 kcal/mol more stable than the reactants! It is interesting to emphasize that formation of **4g** involves the rupture of the original carbon−carbon double bond in ethylene.

In the isomerization pathway between **4c** and **4g**, shown in Figure 8, B^1 in **4c** approaches C^6 and H^3 shifts to C^4 to form the intermediate **4f** through transition state **4tscf**. From **4f**, the insertion of boron into the carbon−carbon bond is completed through transition state **4tsfg**, the overall rate-limiting step for this process. Consequently, despite the great thermodynamic stability of **4g**, its formation is precluded on the basis of kinetic reasons, because **4tsfg** lies about 40 kcal/mol above reactants.

Because of the about 32 kcal/mol exothermicity in the reaction producing **4e** (or compound **3d** in the reaction of BH_2^+ with C_2H_2), it could in principle dissociate to form **3f** and H_2, thus eliminating another H_2 molecule (see Figure 5). However, the required energy for this process is about 58 kcal/mol and, even assuming that all the excess energy remains in **4e**, it cannot dissociate further to **3f**. This is in agreement with experiments, in which addition followed by elimination of only one hydrogen molecule is observed.[1]

The efficiency for this reaction is 0.93, indicating that almost all collisions lead to products.[1] Our calculations indicate that the rate-limiting transition state, **4tsad′**, is 20.2 kcal/mol more stable than the reactants, consistent with such a fast reaction. However, experiments also indicate that 15% of the product is the stabilized adduct. When compared to the reaction of acetylene and despite the fact that both reactions have to surmount limiting transition states with similar energies (actually 4 kcal/mol lower in the ethylene case), the formation of the initial adduct in the reaction with ethylene is not only a slightly less exothermic process but also the energy is distributed between a larger number of degrees of freedom (assuming statistical behavior). Therefore, it should be less probable for the required energy to get localized into the reaction coordinate for the ethylene than for the acetylene reaction. As a consequence, the adduct spends relatively more time in the deep potential well between **4a** and **4c**; therefore, it has more chance to be stabilized by collision with the buffer gas in the SIFT instrument. This interpretation also agrees with the increased H/D scrambling observed experimentally[29] in the reaction of BH_2^+ with C_2D_4.

If complete H/D scrambling occurs in the reaction with C_2D_4, the relative abundance of H_2, HD, and D_2 should be 1:8:6, neglecting kinetic isotope effects. Experimental results[29] show that elimination of H_2, HD and D_2 occurs in a 2.5:8:4.5 proportion. These values are consistent with complete H/D scrambling considering that the slight deviation can account for a small isotope effect favoring the elimination of the lighter molecule. Experiments also show that these results are mirrored in the reaction of BD_2^+ with C_2H_4, which further confirm our interpretation.

As mentioned before, the H/D scrambling occurs during the **4a**−**4c** isomerization. Free rotation along the C^4−C^7 σ bond in **4c** makes H^2, H^8, and H^9 equivalent. Furthermore, the symmetry of **4a** makes equally probable the shift of H^2 to C^7 or H^3 to C^4, and consequently all hydrogen atoms become equivalent. In addition, isomerization through **4b** is also energetically accessible and, therefore, can contribute to the H/D scrambling.

$BH_2^+ + C_2H_6$. The results for this reaction are shown in Table 5 and plotted in Figure 9. From the figure it is evident that our computations suggest that two products can be formed, addition and elimination of H_2 or elimination of CH_4, in excellent agreement with experiments.[1] We also found that more than one pathway for the addition followed by H_2 elimination is possible. One of the paths, **5b**−**5tsbd**−**5d**−**5h**, analogous to the reaction of BH_2^+ with CH_4, has only been mentioned by Depuy in conjunction with the experimental results.[1] Both reactions form initial adducts with similar structures, **5b** and **2a**. They are 39.9 and 32.1 kcal/mol more stable than their reactants, respectively, and the difference in energy is mainly

TABLE 5: Energies, Symmetries, and Number of Imaginary Frequencies for the Reaction of BH_2^+ with C_2H_6

species	symmetry	N_{imag}[a]	MP2(full)/6-311G(d,p) (hartrees)	CCSD(T)/6-311G(d,p)[b] (hartrees)	ZPE[c] (kcal/mol)	rel energy[d] (kcal/mol)
C_2H_6	D_{3d}	0	−79.60859	−79.61565	47.70	
BH_2^+	$D_{\infty h}$	0	−25.55259	−25.55425	11.15	
H_2	$D_{\infty h}$	0	−1.16027	−1.16832	6.48	
5h	C_s	0	−104.04362	−104.04261	47.56	
5g	D_{3d}	0	−104.09460	−104.09215	46.78	
5i	C_{3v}	0	−64.82844	−64.82827	28.80	
CH_4	T_d	0	−40.39804	−40.40582	28.58	
$BH_2^+ + C_2H_6$	N/A	0, 0	−105.16118	−105.16990	58.85	0
5b	C_s	0	−105.23120	−105.23823	61.80	−39.9
5tsbd	C_1	1	−105.18255	−105.18773	58.89	−11.1
5d	C_1	0	−105.21043	−105.21676	58.50	−29.8
5tsdd′	C_1	1	−105.17845	−105.18445	58.15	−9.8
5h + H_2	N/A	0, 0	−105.20389	−105.21093	54.03	−30.6
5tsbc	C_1	1	−105.19362	−105.20027	59.32	−18.6
5c	C_1	0	−105.19493	−105.20392	59.90	−20.3
5tsce	C_1	1	−105.17466	−105.18748	56.80	−13.1
5e	C_s	0	−105.25366	−105.25962	60.80	−54.3
5i + CH_4	N/A	0, 0	−105.22648	−105.23409	57.38	−41.7
5a	C_2	0	−105.24511	−105.24960	62.36	−46.5
5tsae	C_1	1	−105.15778	−105.16764	59.31	1.9
5tsef	C_s	1	−105.21188	−105.21583	58.18	−29.5
5f	C_{2v}	0	−105.25638	−105.26203	54.29	−62.4
5g + H_2	N/A	0, 0	−105.25488	−105.26047	53.26	−62.4

[a] Number of imaginary frequencies. [b] Single point calculation at the MP2(full)/6-311G(d,p) level optimized geometry. [c] Unscaled zero point vibrational energy from MP2(full)/6-311G(d,p) level. [d] Relative energy at the CCSD(T)/6-311G(d,p)//MP2(full)/6-311G(d,p) level including ZPE.

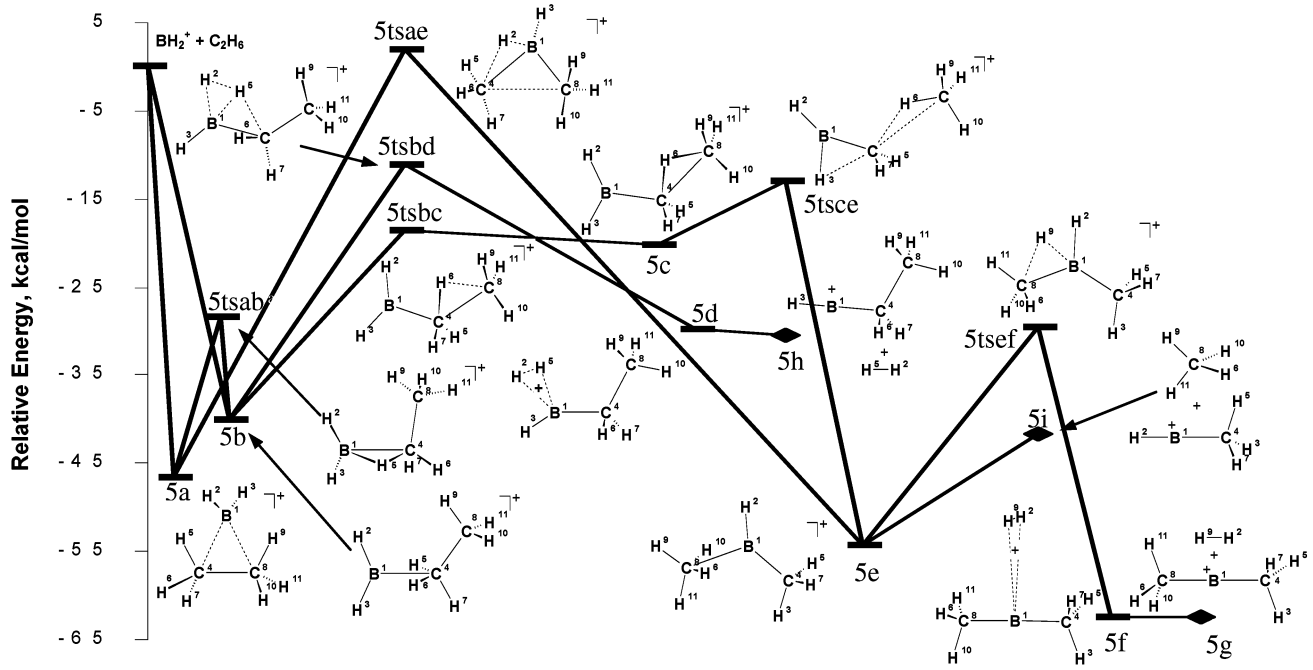

Figure 9. Potential energy surface and structures for the reaction of BH_2^+ with C_2H_6 at the CCSD(T)/6-311G(d,p)//MP2(full)/6-311G(d,p) level including ZPVE.

due to the stabilizing effect of the additional methyl group in **5b**. Complex **5d** is slightly more stable than the products, **5h** and H_2, at our highest level; however, as in the reaction with CH_4, the relative stability is reversed when zero point energy is considered. Therefore, the complex is not bound and the loss of H_2 occurs very quickly. As in the previous reactions, a transition state switching the 3c−2e bond from $B^1-H^2-H^5$ to $B^1-H^2-H^3$ in **5d**, **5tsdd′**, was found (not shown in Figure 9). It has a structure similar to **2tsbb′** and is 19.9 kcal/mol higher than **5d**; therefore, it cannot compete with dissociation.

In addition, another pathway for H_2 elimination was found, i.e., **5a**−**5tsae**−**5e**−**5tsef**−**5f**−**5g**. In contrast to adduct **5b,** in **5a** the boron atom attacks at the center of the C−C bond. Adduct **5a** is more stable than **5b** and is similar in structure to **3a** and **4a**. The stability of these adducts relative to their reactants is in the order **3a** > **4a** > **5a**. From C_2H_2 to C_2H_6 the decreased electron density along the carbon−carbon bond causes the binding energy with BH_2^+ to decrease. Interestingly, AIM analysis performed at MP2(full)/cc-pVTZ level shows that there are three bond critical points and one ring critical point in the $B^1-C^4-C^8$ moiety, as shown in Figure 2G, indicating that $B^1-C^4-C^8$ forms a cyclic structure. In addition, it shows no bonding between B^1-H^5 or B^1-H^9. Structure **5e** is similar to **2a**; however, methane is more loosely bound in the former (12.6

kcal/mol) than in the latter (32.1 kcal/mol) because of the effect of the additional methyl group. The transition state connecting **5a** and **5e**, **5tsae**, is higher in energy than the reactants; therefore, this path is unlikely, which is the only reaction path involving **5a** directly. However, **5a** can easily isomerize to **5b** through transition state **5tsab** and proceed to products via **5tsbd** or/and **5tsbc**. In the last step of this pathway H^9 migrates to B^1 in **5e** to form **5f**, a loose complex of $CH_3BCH_3^+$ and H_2, which lies very close in energy to products and dissociates very quickly to **5g** and hydrogen molecule. In **5f**, the H^2-H^9 bond is 0.74 Å, very close to the equilibrium bond length in H_2 (0.736 Å), whereas the H^2-B^1 and H^9-B^1 bonds are very long, 2.94 Å.

It is interesting to point out that both mechanisms found to eliminate the hydrogen molecule produce ionic products with different structures, which obviously cannot be distinguished in the mass spectrometer. However, our calculations suggest that the structure should be that of **5h**, even though **5g** is about 32 kcal/mol more stable. It seems that in this reaction, as in the reaction with C_2H_4, the generation of a product in which the carbon−carbon bond is broken is thermodynamically favored but kinetically forbidden. In any event, once **5h** is formed, it could in principle isomerize to **5g** after the elimination of H_2 occurs. This isomerization has been investigated in the previous reaction. The results, presented in Figure 8 (right axis) where **5h** and **5g** are identical to **4c** and **4g**, respectively, show that even if all the energy released to form **5h** and H_2 (30.6 kcal/mol) is retained in the ion, it would not be enough to surmount transition state **4tsgf**, around 100 kcal/mol above **5h**.

The channel leading to the loss of methane proceeds through **5b**−**5tsbc**−**5c**−**5tsce**−**5e** and finally generates **5i** and methane. In **5b** H^6 shifts to C^8 and forms minimum **5c**, in which the C^4-C^8 bond breaks through transition state **5tsce**. This transition state is stabilized by the simultaneous formation of the B^1-C^8 and H^3-C^4 bonds that give rise to the only kinetically accessible transition state for the scission of a carbon−carbon bond found in this study.

Compound **5e** is shared by two different pathways, leading to the elimination of either CH_4 or H_2. Although both pathways are energetically feasible, the path to lose H_2 is less probable because it involves **5tsef**, a transition state located 12.3 kcal/mol higher in energy than the methane elimination products (see Figure 9). Moreover, the methane elimination is favored entropically over **5tsef**.

In comparison, in the H_2 elimination pathway (**5b**−**5tsbd**−**5d**−**5h**) the rate-limiting transition state, **5tsbd**, is very close in energy to **5tsce**, the rate-limiting transition state on the methane elimination path (**5b**−**5tsbc**−**5c**−**5tsce**−**5e**−**5i**), in excellent agreement with the experimental branching ratios[1] showing that products for the elimination of H_2 and CH_4 are produced in equal proportions and suggesting that the two pathways compete with each other and occur at about the same speed. In addition, our calculations indicate that transition states **5tsbd** and **5tsce** are 11.1 and 13.1 kcal/mol more stable than the reactants, respectively, suggesting that this reaction should proceed faster than the reactions with H_2 and methane but slower than with acetylene and ethylene, in excellent agreement with the reaction efficiency of 0.82 reported by DePuy.[1]

Experiments on the isotopic labeled reaction BD_2^+ with C_2H_6 show that the loss of HD and CH_4 was observed exclusively.[1] The elimination of HD, analogous to the reaction with methane, involves the path **5b**−**5tsbd**−**5d**−**5h**, in which the hydrogen molecule H^2-H^5 is formed (Figure 9). In H^5-H^2, H^2 is from BH_2^+ and H^5 is from C_2H_6; thus only HD is formed in the reaction of BD_2^+, in excellent agreement with experiments. We should also point out that the path leading to the elimination of H_2 with **5g** as final product should also produce HD in the labeled reaction (see Figure 9); however, as discussed above, it might not play a role because elimination of methane is favored once **5e** is formed. In the elimination of CH_4, path **5b**−**5tsbc**−**5c**−**5tsce**−**5e**−**5i**, the leaving methane contains H^6, H^9, H^{10}, and H^{11}. All the hydrogen atoms in methane are from reactant ethane; thus, the reaction of BD_2^+ with ethane should produce CH_4 exclusively, in agreement with experimental results. Furthermore, no structures that could produce H/D scrambling were found in this pathway.

Conclusions

The reactions of BH_2^+ studied here show the remarkable electrophilic characteristics of BH_2^+. It is less reactive than CH_3^+, but substantially more selective too, as evidenced by the reactions of BD_2^+. The theoretical results suggest reaction mechanisms that are in complete agreement with known experimental data.

The reactions of BH_2^+ with simple hydrocarbons show that very exothermic adducts are formed and that the stability of these adducts depends on the availability of electron rich bonds in the hydrocarbon; therefore, their relative stability is acetylene > ethylene > ethane. This is also the order of reactivity as revealed by the relative energy of the rate limiting transition state for each reaction and in agreement with experiments. The AIM and natural bond analyses show some insights into the bonding structure of the adducts and suggest structures ranging from clearly cyclic in ethane to "T" shaped as in the case of acetylene.

The rupture of a carbon−hydrogen bond occurs in all the reactions studied and H_2 is the common elimination product, similar to the reaction of some transition state cations. In contrast, the carbon−carbon bond is activated only in ethane despite a very exothermic reaction in acetylene and ethylene is predicted.

Acknowledgment. This work was supported by the University of Idaho, the Idaho NSF-EPSCoR, and the Research Corporation through a Research Innovation Award.

References and Notes

(1) DePuy, C. H.; Gareyev, R.; Hankin, J.; Davico, G. E.; Krempp, M.; Damrauer, R. *J. Am. Chem. Soc.* **1998**, *120*, 5086.
(2) DePuy, C. H.; Gareyev, R.; Hankin, J.; Davico, G.; Damrauer, R. *J. Am. Chem. Soc.* **1997**, *119*, 427.
(3) Salzbrunn, S.; Rasul, G.; Prakash, G. K. S.; Olah, G. A. *J. Mol. Model.* **2000**, *6*, 213.
(4) Rasul, G.; Olah, G. A. *Inorg. Chem.* **1997**, *36*, 1278.
(5) Weisshaar, J. C. *Acc. Chem. Res.* **1993**, *26*, 213.
(6) Eller, K.; Schwarz, H. *Chem. Rev.* **1991**, *91*, 1121.
(7) Kemper, P. R.; Bushnell, J. E.; Weis, P.; Bowers, M. T. *J. Am. Chem. Soc.* **1998**, *120*, 7577.
(8) Nichols, J.; Gutowski, M.; Cole, S. J.; Simons, J. *J. Phys. Chem.* **1992**, *96*, 644.
(9) Sharp, S. B.; Gellene, G. I. *J. Am. Chem. Soc.* **1998**, *120*, 7585.
(10) Ranatunga, T. D.; Kennady, J. M.; Kenttamaa, H. I. *J. Am. Chem. Soc.* **1997**, *119*, 5200.
(11) Rasul, G.; Prakash, G. K. S.; Olah, G. A. *J. Am. Chem. Soc.* **1999**, *121*, 7401.
(12) McDonald, L. E.; Gellene, G. I. *Mol. Phys.* **2001**, *99*, 377.
(13) Qu, Z.-W.; Zhu, H.; Li, Z.-S.; Zhang, Q.-Y. *Chem. Phys. Lett.* **2001**, *339*, 140.
(14) Qu, Z. W.; Li, Z. S.; Ding, Y. H.; Sun, C. C. *Chem. J. Chin. Universities* **2001**, *22*, 1711.
(15) Olah, G. A.; Prakash, G. K. S.; Rasul, G. *Arkivoc* **2002**, 7.
(16) Kemper, P. R.; Bushnell, J.; Bowers, M. T.; Gellene, G. I. *J. Phys. Chem. A* **1998**, *102*, 8590.
(17) Bader, R. F. W. *Atoms in Molecules: A Quantum Theory*; Oxford University Press: Oxford, U.K., 1994.

(18) Bader, R. F. W. *Acc. Chem. Res.* **1985**, *18*, 9.
(19) Frisch, M. J.; Trucks, G. W.; Schlegel, H. B.; Scuseria, G. E.; Robb, M. A.; Cheeseman, J. R.; Zakrzewski, V. G.; Montgomery, J. A.; Stratmann, R. E.; Burant, J. C.; Dapprich, S.; Millam, J. M.; Daniels, A. D.; Kudin, K. N.; Strain, M. C.; Farkas, O.; Tomasi, J.; Barone, V.; Cossi, M.; Cammi, R.; Mennucci, B.; Pomelli, C.; Adamo, C.; Clifford, S.; Ochterski, J.; Petersson, G. A.; Ayala, P. Y.; Cui, Q.; Morokuma, K.; Malick, D. K.; Rabuck, A. D.; Raghavachari, K.; Foresman, J. V.; Cioslowski, J.; Ortiz, J. V.; Baboul, A. G.; Stefanov, B. B.; Liu, G.; Liashenko, A.; Piskorz, P.; Komaromi, I.; Gomperts, R.; Martin, R. L.; Fox, D. J.; Keith, T.; Al-Laham, M. A.; Peng, C. Y.; Nanayakkara, A.; Gonzales, C.; Challacombe, M.; Gill, P. M. W.; Johnson, B.; Chen, W.; Wong, M. W.; Andres, J. L.; Head-Gordon, M.; Replogle, E. S.; Pople, J. A. *Gaussian 98*, Revision A.9; Gaussian, Inc.: Pittsburgh, PA, 1998.
(20) We would like to thank Dr. Christopher Hadad for providing the code written originally by Paul Rablen.
(21) Gareyev, R.; DePuy, T. J.; Bierbaum, V. M.; DePuy, C. H. *Int. J. Mass Spectrom.* **1998**, *180*, 55.
(22) Rasul, G.; Prakash, G. K. S.; Olah, G. A. *J. Phys. Chem. A* **2000**, *104*, 2284.
(23) Rasul, G.; Prakash, G. K. S.; Olah, G. A. *Proc. Natl. Acad. Sci. U.S.A.* **2002**, *99*, 13387.
(24) Gioumousis, G.; Stevenson, D. P. *J. Chem. Phys.* **1958**, *29*, 294.
(25) Chesnavich, W. J.; Su, T.; Bowers, M. T. *J. Chem. Phys.* **1980**, *72*, 2641.
(26) Bell, C. J.; Gellene, G. I. *Faraday Discuss.* **2001**, *118*, 477.
(27) Byun, Y. G.; Saebo, S.; Pittman, C. U., Jr. *J. Am. Chem. Soc.* **1991**, *113*, 3689.
(28) Andrews, L.; Lanzisera, D. V.; Hassanzadeh, P.; Hannachi, Y. *J. Phys. Chem. A* **1998**, *102*, 3259.
(29) Hankin, J.; Davico, G.; DePuy, C. H.; Damrauer, R. Unpublished results.